Spin-polarized self-consistent local orbital method and its application to ferromagnetic Ni(001) slabs
by Xueyuan Zhu

A thesis submitted in partial fulfillment of the requirements for the degree of Doctor of Philosophy in Physics
Montana State University
© Copyright by Xueyuan Zhu (1983)

Abstract:
The electron structure and magnetism of one, three and five-layer Ni(001) slabs are calculated by our spin-polarized adaptation of the self-consistent local orbital method developed by Arlinghaus, Gay and Smith. A new correlation potential derived from a recent analysis of correlation energy for the spin-polarized electron liquid by Vosko, Wilk and Nusair, has been employed in these calculations. The magnetic moments of the surface-layers are 0.98, 0.69 and 0.65 *mu;B/atom for these three slabs, respectively. At the inner planes of tnree and five-layer slabs the bulk moment limit (0.56 μB/atom) are approached due to the increased atomic coordinations. The contributions of dehybridization and band-narrowing to this "surface magnetism enhancement" have been determined by repeating the calculations with sp-d matrix elements omitted. The results show that the dehybridization only plays a minor role.

SPIN-POLARIZED SELF-CONSISTENT LOCAL ORBITAL METHOD

AND ITS APPLICATION TO FERROMAGNETIC Ni(001) SLABS

by

Xueyuan Zhu

A thesis submitted in partial fulfillment
of the requirements for the degree

of

Doctor of Philosophy

in

Physics

MONTANA STATE UNIVERSITY
Bozeman, Montana

August 1983

ii

APPROVAL

of a thesis submitted by

Xueyuan Zhu

This thesis has been read by each member of the thesis committee and has been found to be satisfactory regarding content, English usage, format, citations, bibliographic style, and consistency, and is ready for submission to the College of Graduate Studies.

August 1, 1983
Date

John Hernandez
Chairman, Graduate Committee

Approved for the Major Department

August 1, 1983
Date

_____
Head, Major Department

Approved for the College of Graduate Studies

12 Aug. 1983
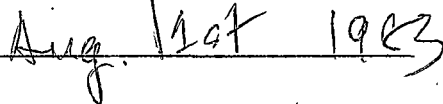Date

Michael Malone
Graduate Dean

iii

STATEMENT OF PERMISSION TO USE

In presenting this thesis in partial fulfillment of the require-
ments for a doctoral degree at Montana State University, I agree that
the Library shall make it available to borrowers under rules of the
Library. I further agree that copying of this thesis is allowable only
for scholarly puposes, consistent with "fair use" as prescribed in
the U.S. Copyright Law. Requests for extensive copying or repro-
duction of this thesis should be referred to University Microfilms
International, 300 North Zeeb Road, Ann Arbor, Michigan 48106, to
whom I have granted "the exclusive right to reproduce and distribute
copies of the dissertation in and from microfilm and the right to
reproduce and distribute by abstract in any format."

Signature _____
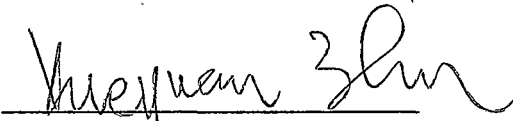
Date _____

ACKNOWLEDGEMENTS

TABLE OF CONTENTS

LIST OF FIGURES

LIST OF TABLES

ABSTRACT

The electron structure and magnetism of one, three and five-layer Ni(001) slabs are calculated by our spin-polarized adaptation of the self-consistent local orbital method developed by Arlinghaus, Gay and Smith. A new correlation potential derived from a recent analysis of correlation energy for the spin-polarized electron liquid by Vosko, Wilk and Nusair, has been employed in these calculations. The magnetic moments of the surface-layers are 0.98, 0.69 and 0.65 μ_B/atom for these three slabs, respectively. At the inner planes of three and five-layer slabs the bulk moment limit (0.56 μ_B/atom) are approached due to the increased atomic coordinations. The contributions of dehybridization and band-narrowing to this "surface magnetism enhancement" have been determined by repeating the calculations with sp-d matrix elements omitted. The results show that the dehybridization only plays a minor role.

1

CHAPTER I

INTRODUCTION

Recently, the number of experimental and theoretical studies of magnetism on d-band metal surfaces has increased very rapidly, due to the development of promising new techniques for detecting electron spin-polarization on surfaces, including photoemission (Ref.1-4), tunneling (Ref.5), field-emission spectroscopies (Ref.6-7), scattering of spin-polarized electrons (Ref.8), electron-capture spectroscopy (Ref. 9-10), Hall-effect measurements (Ref.11), and ferromagnetic resonance (Ref.12).

Magnetism is one of the most fundamental and technologically important physical phenomena. The theoretical interest of surface magnetism has attracted more and more theorists during the past several years. The succesful local spin-density approximation and the full self-consistent methods for electronic band structure provide great opportunities in this new area.

In the early 70's, there were some very interesting but contradictory measurements on very thin ferromagnetic slabs and interfaces. Liebermann et al. (Ref.19) reported "dead" magnetism for less than about 2.5 layers of Ni deposited on a Cu substrate.

Bergmann's (Ref.11) anomalous Hall effect measurement supported the existence of "dead" layers. But the spin polarized photoemission measurement by Pierce et al. (Ref.8) showed that even a Ni monolayer deposited on Cu is magnetized. Rau's (Ref.9-10) electron capture spectroscopy measurement agreed with this, but pointed out that the magnetism of Ni overlayer has a reduced moment.

Stoner first proposed the band-structure theory of magnetism (Ref.20-21). C. S. Wang and J. Callaway succesfully realized a self-consistent spin-polarization calculation for bulk Ni (Ref.22).

A thin film is somewhat different from a real semi-infinite surface; however, a thick enough thin-film model can accurately simulate the surface properties with great convenience in computation.

In 1980, C. S. Wang and Freeman (Ref.23-24) first used a self-consistent LCAO method to calculate the magnetism of a 9-layer Ni(100) slab. They did not find any magnetically "dead" layers, but a 20% surface-moment deficit ($0.44\mu_B$) compared with the bulk-like central-layer moment. They attributed this deficit to a vacancy of a majority-spin $\bar{M}_3$ surface state.

Recently, Jepsen, Madsen and Andersen (Ref.25-26) reported the results for the magnetic behvior of one (Ni1), three (Ni3) and five-layer (Ni5) slabs of Ni(100) computed by the LAPW method. In the 5-layer slab case, the magnetic moment of each layer was 0.61, 0.55 and 0.65 μ_B from central to surface layer. This result shows

10% enhancement of the surface magnetism compared with the central layer. They obtained an unoccupied $\bar{M}_3$ majority-spin surface state, but they believe it was not enough to cause a surface magnetic deficit. They pointed out: "The essential mechanism behind this is the narrowing at the surface of the $3z^2$-r^2, xz and yz bands and the broadening of the x^2-y^2 and xy bands." They predicted: "The spin moment at the (100) surface of a Ni crystal is enhanced over the bulk value by roughly 10% to about 0.63 μ_B per atom, and the enhancement is mostly of $E_g(x^2$-$y^2)$ character, and to a small extent, $T_{2g}(xy)$ character."

. D. S. Wang, Krakauer and Freeman have used a LAPW method and presented some newer results of Ni(001) and Ni(110) slabs (Ref. 27-28). They claimed that they also found surface magnetism enhancement which is due to a full majority-spin $\bar{M}_3$ surface state.

Some other groups computed the magnetism of Ni/Cu, Cu/Ni interfaces and Ni(100) monolayer (Ref.29-31).

Starting in the summer of 1981, we adopted the SCLO method (Ref. 32-34) of Smith, Gay and Arlinghaus of General Motor Research Laboratories, and succesfully calculated one, three and five-layer slabs of Ni(100). The results agreed excellently with Jepsen et al.

Plummer et al. and Erskine (Ref.35-37) published their spin-polarized photoemission results for the Ni(100) surface. They pointed

out the existence of some surface states. Some of these surface states had been predicted by Dempsey and Kleinman (Ref.38) previously. Unfortunately until now there has been no way to distinguish the magnetic moments of different layers.

CHAPTER 2

METHODOLOGY

Exchange and Correlation (XC) Potentials

In single electron theory, the many-body effect is approximated by a mean field. Hartree and Fock(HF) (Ref.39-40) first introduced the "exchange potential," which is due to the anti-symmetric exchange property of the wavefunction of a spin-1/2 particle system. Their method is called the HF approximation, and the exchange energy or potential is named the HF energy or potential.

The "correlation energy" of an interacting electron gas is defined as the difference between the HF energy and any better approximation to the total energy. So, the total potential of a single electron is, combining the potentials,

$$V^{\sigma}(\tilde{r}) = \Phi(\tilde{r}) + V_X^{\sigma}(\tilde{r}) + V_C^{\sigma}(\tilde{r}) \tag{1}$$

where $\Phi(\tilde{r})$ is the electrostatic potential

$$\Phi(\tilde{r}) = \int \frac{\rho(\tilde{r}')}{|\tilde{r}-\tilde{r}'|} d\tilde{r}' - \sum_{\tilde{m}} \frac{Z}{|\tilde{r}-\tilde{m}|} \tag{2}$$

In local-spin-density theory (Ref.41-43), the exchange energy

can be written as

$$\varepsilon_x = \varepsilon_x(r_s, \zeta) \tag{3}$$

where

$$r_s = (3/4\pi\rho)^{1/3} , \quad \rho(\tilde{r}) = \rho_+(\tilde{r}) + \rho_-(\tilde{r}) , \tag{4}$$

and

$$\zeta = (\rho_+ - \rho_-)/(\rho_+ + \rho_-) \tag{5}$$

Thus, the exchange potential will be

$$V_x^\sigma = \frac{\partial}{\partial\rho_\sigma}(\rho\varepsilon_x) = \varepsilon_x + \rho\frac{\partial\varepsilon_x}{\partial r_s}\frac{\partial r_s}{\partial\rho_\sigma} + \rho\frac{\partial\varepsilon_x}{\partial\zeta}\frac{\partial\zeta}{\partial\rho_\sigma} \tag{6}$$

Since

$$\rho\frac{\partial r_s}{\partial\rho_\sigma} = -\frac{r_s}{3} \tag{7}$$

and

$$\rho\frac{\partial\zeta}{\partial\rho_\pm} = \pm(1 \mp \zeta) , \tag{8}$$

The exchange energy is given by an analytic form

$$V_x^{\pm} = \varepsilon_x - \frac{r_s}{3}\frac{\partial \varepsilon_x}{\partial r_s} \pm (1\mp\zeta)\frac{\partial \varepsilon_x}{\partial \zeta} \tag{9}$$

This tells us that the exchange energy favors a ferromagnetic ground state in which the imbalance between ρ_+ and ρ_- would decrease the total energy of the system.

For $\rho_+ = \rho_-$, we introduce the paramagnetic exchange energy

$$\varepsilon_x^P = -\frac{3}{2}\left(\frac{3}{\pi}\right)^{1/3}\rho^{1/3} \tag{10}$$

Then Eq(9) becomes

$$\varepsilon_x^{\pm} = \varepsilon_x^P(1\pm\zeta)^{1/3} \tag{11}$$

The exchange energy per electron at a certain spatial point, where the density ρ and polarization ζ are defined, is

$$\varepsilon_x(r_s,\zeta) = \varepsilon_x^P(r_s)\{(1+\zeta)^{4/3} - (1-\zeta)^{4/3}\}/2 \tag{12}$$

Since

$$\varepsilon_x - \frac{r_s}{3}\frac{\partial \varepsilon_x}{\partial r_s} = \frac{4}{3}\varepsilon_x(r_s,\zeta)$$

$$(1\pm\zeta)\frac{\partial \varepsilon_x}{\partial \zeta} = \frac{2}{3}\varepsilon_x^P(1\pm\zeta)\{(1+\zeta)^{1/3} - (1-\zeta)^{1/3}\}, \tag{13}$$

the exchange potential is

$$V_{\overline{x}}^{+} = \frac{4}{3} \, \varepsilon_x^P (1\underline{\pm}\zeta)^{1/3} = -2(3\rho_{\underline{+}}/\pi)^{1/3} \tag{14}$$

Kohn and Sham (Ref.44) first obtained this result in 1965. We may notice that it is only 2/3 of Slater's exchange potential (Ref.45) which overestimated the exchange effect and caused unreasonably large theoretical values of magnetic moments (Ref.46-48).

In the 1930's, Wigner (Ref.49-50) calculated the correlation energy for both high and low-density limits of a paramagnetic electron system. Pines (Ref.51-52) first suggested an interpolation formula

$$\varepsilon_c = \frac{-0.88}{r_s + 7.8} \tag{15}$$

for the metallic density (1.9< r_s <5.6). Thus, one can obtain a corresponding Wigner potential for paramagnetic system.

$$V_c = \frac{d}{d\rho} (\rho \varepsilon_c) = - \frac{0.56\rho^{2/3} + 0.0059\rho^{1/3}}{(0.079 + \rho^{1/3})^2} \tag{16}$$

We adapted the correlation energy from a recent study of the spin-polarized electron liquid by Vosko, Wilk and Nusair (Ref.53). They used a Pade method to interpolate the correlation energy data from the high to low-density regions, where the results of the RPA (Ref. 54-56) and Monte Carlo methods, (Ref.57) are available, respectively.

We suppose the spin-dependent correlation energy can be written as

$$\varepsilon_c(r_s,\zeta) = \varepsilon_c(r_s,0) + \frac{1}{2}\alpha_c(r_s)\zeta^2 \qquad (17)$$

and both $\varepsilon_c(r_s,o)$ and $\alpha_c(r_s)$ can be interpolated as

$$\varepsilon_c(r_s,0) = -AF(r_s/R) \qquad (18)$$

$$\alpha_c(r_s) = A_\alpha F(r_s/R_\alpha) \qquad (19)$$

where

$$F(x) = (1+x^3)\ln(1+\frac{1}{x}) \qquad (20)$$

Since

$$F(x) - \frac{x}{3}F'(x) = \ln(1+\frac{1}{x}) \qquad (21)$$

The spin-polarized correlation potential becomes

$$V_c = -A\ln(1+\frac{R}{r_s}) + \alpha_c(r_s)\zeta + \beta_c(r_s)\zeta^2 \qquad (22)$$

where

$$\beta_c(r_s) = \frac{1}{2}A_\alpha \ln(1+\frac{R}{r_s}) - \alpha(r_s) \qquad (23)$$

We find A=48.6 mRyd, R=15, and A_α=31.1 mRyd, R_α=16.4 which can fit Vosko's data for ε_c and α_c to better than 1 mRyd.

Table 1. The paramagnetic correlation energy (mRyd)

of Vosko et al, and Zhu-Hermanson's fit

with A=48.6 mRyd and R=15

r_s	Vokso et al	Zhu-Hermanson
0.5	154.13	151.4
1.0	120.04	120.0
2.0	89.57	90.2
3.0	73.77	74.5
4.0	63.57	62.5
5.0	56.27	56.4
10.0	37.09	36.1

Table 2. The spin-stiffness of the correlation

energy (mRyd), $\alpha_c(r_s)$, of Vosko et al,

Zhu-Hermanson, and von Barth-Hedin

r_s	Vosko et al	Zhu-Hermanson[*]	von Barth-Hedin
0.5	100.1	99.6	122.7
1.0	79.4	79.4	94.7
2.0	60.1	60.2	68.2
3.0	49.8	49.9	53.7
4.0	43.0	43.0	44.2
5.0	38.0	38.0	37.3
6.0	34.2	34.2	32.0

* Zhu-Hermanson's fit uses the parameters

$$A_\alpha = 31.1 \text{ mRyd}$$

and

$$R_\alpha = 16.4.$$

We can expand the exchange potential as

$$V_{\overline{x}}^{\pm} = V_x^P(1 \pm \frac{1}{3}\zeta + \frac{1}{9}\zeta^2 + \cdots) \tag{24}$$

From Eq(22) and Eq(24), we find that the XC potential difference between up and down-spin is

$$\Delta V_{xc} = \Delta V_x + \Delta V_c \tag{25}$$

where

$$\Delta V_x = -\frac{2}{3}V_x^P(r_s)\zeta \tag{26}$$

$$\Delta V_c = 2\alpha_c(r_s)\zeta \tag{27}$$

This shows that the exchange potential favors spin-polarization but the correlation potential opposes this tendency. The final balance between these two competing potentials will build up a stable magnetic moment in some metals.

Comparing our data with the commonly used von Barth-Hardin (BH) correlation potential, we find that the BH potential over-estimates the spin-polarization stiffness α_c at the most important density region ($0.5 < r_s < 2.0$) for Ni. For Ni1, we tested both the Vosko and BH potentials and we find that the BH potential leads to a reduction of the magnetic moment, by 1%, and a reduction of the spin-splitting, by 2-8% (Ref.58).

Geometry and Symmetry

Because of the existence of a surface, the 3-D periodicity of the bulk structure will be broken in the z-direction which is perpendicular to this surface. If we use a periodically-repeated thin-slab model to simulate the bulk-surface system, then we can recover the periodicity in the z-direction and employ the Fourier transformation technique again. Thus the problem will be much simpler mathematically than that of a real semi-infinite system.

Essentially, a Ni5 slab is good enough to describe a surface system, since the central layer's features are very close to the bulk's. Usually, we assume the distance between two slabs, "ELZ", to be about 10 times the lattice constant, "ALAT", of the surface structure. Thus, we have determined a 3-D unit cell with a volume of $ALAT^2*ELZ$. Inside this unit cell, the number of atoms is equal to the number of layers comprising the slab.

On the Ni(001) surface, the x and y axes are defined to be along the bulk [100] and [010] directions as shown in Fig.1.

In this real space coordinate system, we ordered the atomic orbitals of each layer as below:

1.	1s	13.	3d(yz)
2.	2s	14.	$3d(x^2-y^2)$
3.	2p(x)	15.	4s
4.	2p(y)	16.	4p(x)

5. 2p(z)	17. 4p(y)
6. 3s	18. 4p(z)
7. 3p(x)	19. 5s
8. 3p(y)	20. $4d(3z^2-r^2)$
9. 3p(z)	21. 4d(xy)
10. $3d(3z^2-r^2)$	22. 4d(xz)
11. 3d(xy)	23. 4d(yz)
12. 3d(xz)	24. $4d(x^2-y^2)$

In this coordinate system the $\bar{\Sigma}$ line is parallel to the x axis and the $\bar{\Delta}$ line is at 45° (see Fig.1). Our symmetry labels conform to the character table of Alldredge and Kleinman (Ref.59). We add primes to denote the odd symmetries under z-reflection.

Because of the symmetry property, we only need to consider the 1/8 irreducible region of the square Brillouin zone. To study the magnetism of the slab, we calculated the charge densities of both spins by summing the square of wavefunctions over 15 or 36k points in the irreducible zone:

$$\rho^\sigma(\tilde{r}) = \sum_{i}^{Ei<E_F} \sum_{k_{11}} | \psi^\sigma_{i,k_{11}}(\tilde{r}) |^2 \tag{28}$$

The 15 and 36k point samples are shown in Fig. 2.

For the Ni(100) slab, the point group is D_{4h}, i.e., $(C_{4v}*R_z)$, where C_{4v} is the square group and R_z is a z-reflection group with 2

elements, I and σ_z. The operations of these 2 elements are

$$I : \quad x \quad y \quad z$$

$$\sigma_z: \quad x \quad y \quad -z$$

C_{4v} has 8 elements in 5 classes. Their operations are

$$I : \quad x \quad y \quad z$$

$$C_4^2: \quad -x \quad -y \quad z$$

$$2C_4^1: \quad -y \quad x \quad z$$

$$\quad\quad\quad y \quad -x \quad z$$

$$2\sigma_{x,y}: \quad x \quad -y \quad z$$

$$\quad\quad : \quad -x \quad y \quad z$$

$$2\sigma_{x\pm y}: \quad -y \quad -x \quad z$$

$$\quad\quad\quad y \quad x \quad z$$

In k-space, the wavevector group (Ref.60) of the high-symmtry points and lines are

$\bar{\Gamma}$, $\bar{M}$:　$\{$ I, C_4^2, $2C_4^1$, $2\sigma_{x,y}$, $2\sigma_{x\pm y}$ $\}*\{$ I,σ_z $\}$

$\bar{X}$:　$\{$ I, C_4^2, σ_{x+y}, σ_{x-y}, $\}*\{$ I, σ $\}$

$\bar{\Delta}$:　$\{$ I,σ_{x-y} $\}*\{$ I,σ_z $\}$

$\bar{\Sigma}$:　$\{$ I, σ_x $\}*\{$ I, σ_z $\}$

$\bar{Y}$:　$\{$ I,σ_{x+y} $\}*\{$ I,σ_z $\}$

However, there is only R_z symmtry for general k_{11} points.

At $\bar{\Gamma}$ and $\bar{M}$, there is C_{4v} symmtry plus R_z. The irreducible

representations and basis functions of C_{4v} are (Ref.61).

$$\bar{\Gamma}_1, \bar{M}_1 : 1; z; 3z^2-r^2$$

$$\bar{\Gamma}_2, \bar{M}_2 : xy(x^2-y^2)$$

$$\bar{\Gamma}_3, \bar{M}_3 : xy$$

$$\bar{\Gamma}_4, \bar{M}_4 : x^2-y^2$$

$$\bar{\Gamma}_5, \bar{M}_5 : x, y; xz, yz$$

For a Ni(001) slab with more than one layer, there are two types of plane, A and B, which are displaced by a vector $\tilde{n}_o$ with respect to each other (see Fig. 1). For the A-plane, one of the lattice points is defined at the origin. We emphasize that the basis function $xy(x^2-y^2)$ of the $\bar{M}_2$ symmetry has the same symmetry as B-plane's xy band at the $\bar{M}$ point (see Fig. 3). But the A-plane's xy band at $\bar{M}$ point belongs to $\bar{M}_3$ symmetry. This was pointed out in Ref.59.

For the X point, there is C_{2v} symmetry plus R_z; its representations and basis functions are

$$\bar{X}_1 : 1; z; xy; 3z^2-r^2$$

$$\bar{X}_2 : x+y; x-y; x^2-y^2$$

$$\bar{X}_3 : (x+y)z$$

$$\bar{X}_4 : (x-y)z$$

In addition to R_z reflection symmetry, there are other mirror-plane reflection σ_{x-y}, σ_x and σ_{x+y} for high symmetry lines $\bar{\Delta}$, $\bar{\Sigma}$ and $\bar{Y}$ respectively. We will denote with 1 even xy-parity functions,

and with 2 those odd on these lines. Since all symmetrical and general points have σ_z reflection symmetry, we are able to separate the Hamiltonian and overlap matrixes into even and odd parts, reducing the diagnoalization time by a factor of four.

Atomic Orbitals, Potentials and Preliminary Calculation

Because of the localization of d-electrons, the atomic orbital basis is a reasonable choice for d-band metals calculations. To simplify the calculation of Hamiltonian and overlap matrix elements, our localized atomic orbitals are restricted to be linear combinations of Gaussians of various angular momenta.

$$a_i(\tilde{r}) = Y_{\ell m}(\Theta,\phi) r^\ell \sum_j D_j(i) \exp\{-\alpha_j(i) r^2\} \tag{29}$$

For Ni or Cu, we built a minimum basis set with 15 occupied atomic orbitals, 1s, 2s, 2p, 3s, 3p, 3d and 4s for each layer, which have been expanded into linear combinations of Gaussians. To increase the variational freedom, three diffuse single Gaussians are added to simulate the virtual orbitals, 5s, 4p and 4d, in the outer atomic region. Since our basis of 24 functions per layer is much smaller than that used in LAPW calculations for Ni slabs(45-55/layer), a considerable reduction of computing time is realized.

The procedure for computing the coefficients $D_j(i)$ and scale factors $\alpha_j(i)$ of different orbitals is described in Ref. 62 and the

App. A of Ref. 32. In Table 3., we list the scale factors α_j and coefficients D_j of s, p, and d orbitals respectively.

The starting potential for the calculations is made by overlapping atomic-charge densities. In computing the matrix elements of this potential, it is expedient to first compute the matrix elements of a potential made up of overlapping (spherically symmetric) atomic potentials

$$W(\tilde{r}) = \sum_{\tilde{m}} v(\tilde{r}-\tilde{m}) \tag{30}$$

where $v(\tilde{r}-\tilde{m})$ is the atomic potential and the sum runs over all atomic sites denoted by position vector $\tilde{m}$. The atomic potential consists of a nuclear term plus an electronic term

$$v(r) = -\frac{Z}{r} + u_e(r) \tag{31}$$

To eliminate the divergent behavior of the nuclear term, we construct a "total atomic potential"

$$u(r) = \frac{Z}{r} \{\exp(-r^2)-1\} + u_e(r) \tag{32}$$

which has no singularity at the origin and is suitable for approximation by a Gaussian expansion. Thus, the potential of Eq(31) can be

Table 3-1. The scale factors α_j

and coefficients D_j for s orbitals

α_j	D_j of 1s	D_j of 2s	D_j of 3s	D_j of 4s
0.0700000	0.0000000	0.0000000	0.0000000	0.0000000
0.1197705	0.0000000	0.0000000	0.0000000	0.6124116
0.3348712	0.0000000	0.0000000	0.0000000	-0.1321180
0.9677963	0.0000000	0.0000000	-1.7346211	-0.8146539
2.8920765	0.0000000	0.0000000	-3.6407412	-1.3487436
8.0913675	0.0000000	8.1439547	7.1295201	2.1434983
22.9389906	0.0000000	13.6110435	7.9676855	2.0088771
84.7615438	-33.5437246	-20.6783054	-8.8727049	-2.1661321
308.8317048	-88.6403776	-35.5545761	-13.8704636	-3.7633698
1125.2393196	-74.2300154	-23.3222079	-8.9912178	-2.0093845
4099.8495514	-41.1512705	-12.7762859	-4.8537313	-1.6512891
14937.9479113	-32.2048517	-9.4898366	-3.6259127	-0.5712576

* For 5s, there is only a nonzero coefficient D_1=0.3438588.